DOI: 10.1111/jiec.13293

RESEARCH ARTICLE

JOURNAL OF INDUSTRIAL ECOLOGY WILEY

Life-cycle energy and environmental emissions of cargo ships

Yiqi Zhang[1] | Yuan Chang[2] | Changbo Wang[3] | Jimmy C. H. Fung[1] | Alexis K. H. Lau[1]

[1]Division of Environment and Sustainability, The Hong Kong University of Science and Technology, Hong Kong, China

[2]School of Management Science and Engineering, Central University of Finance and Economics, Beijing, China

[3]College of Economics and Management & Research Center for Soft Energy Science, Nanjing University of Aeronautics and Astronautics, Nanjing, China

Correspondence
Yiqi Zhang, Division of Environment and Sustainability, The Hong Kong University of Science and Technology, Hong Kong, China.
Email: yzhangen@connect.ust.hk
Yuan Chang, School of Management Science and Engineering, Central University of Finance and Economics, Beijing, China. Email: yuan.chang@cufe.edu.cn.

Editor Managing Review: Ian Vázquez-Rowe

Funding information
Central University of Finance and Economics, Grant/Award Number: QYP202107; Research Grants Council, University Grants Committee, Grant/Award Number: PDFS2122-6S09

Abstract

Maritime shipping is under increasing pressure to alleviate its environmental impact. To this end, life-cycle footprint accounting provides a foundation for taking targeted measures in the green transition of shipping. This study used the process-based hybrid life-cycle inventory (LCI) modeling approach to estimate the "cradle-to-propeller" footprint of ships, including primary energy consumption, carbon dioxide emissions, and sulfur dioxide emissions. We used the input–output LCI model to calculate the embodied energy and emissions associated with the material and fuel use of ship manufacturing. We used a bottom-up emission model and global marine traffic data to estimate the operational footprint of different types of ships. Based on 382 cargo ships (including bulk carriers, container ships, and general cargo ships) constructed in mainland China between 2011 and 2015, we estimated that the embodied footprint accounted for <10% of the cradle-to-propeller footprint under the pre-2019 policy scenario. In terms of life-cycle energy intensity (MJ/nm/1000 deadweight tonnage [DWT]), the large bulk carrier (>100,000 DWT) establishes the lowest value (46), followed by the small (0–100,000 DWT) bulk carrier (96), the large container ship (133), the small container ship (196), and the small general cargo (238). The bulk carrier was identified as the most energy efficient among the three ship types, and ships with larger capacities (i.e., DWT) had higher energy efficiencies than ships with lower capacities. Our study provides a comprehensive understanding of the life-cycle footprints of cargo ships, thus enabling better evidence-based policymaking to transition the global marine-shipping industry to a future of greener energy.

KEYWORDS
cargo ship, environmental emissions, footprint accounting, hybrid life-cycle inventory, industrial ecology, input–output analysis

1 | INTRODUCTION

Maritime shipping transports approximately 80—90% of international trade (UNCTAD, 2018). As the global transition toward a low-carbon and clean-air future becomes urgent, maritime shipping is under increasing pressure to alleviate its environmental impact. In April 2018, the International Maritime Organization (IMO) embarked on a decarbonization initiative for international shipping, aiming to reduce carbon emissions by at least 50% by 2050 relative to 2008 (IMO, 2018). In addition to being a climate change mitigation strategy, the regularization of low-carbon

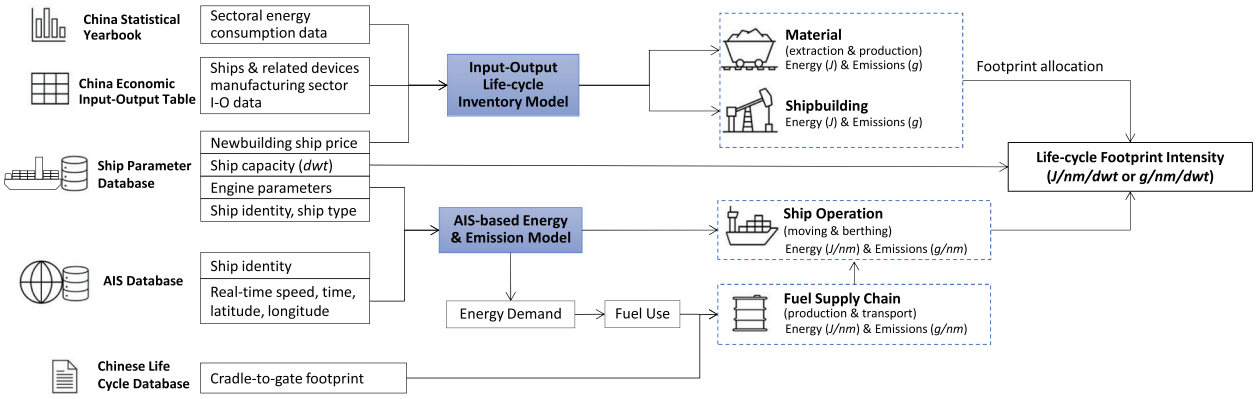

FIGURE 1 Estimation framework

maritime shipping also provides global momentum for reforming the long-term energy system of the sector by adopting alternative fuels and cleaner technologies (Olmer et al., 2017). Therefore, it is of interest to investigate the energy use and atmospheric emissions of a vessel over its entire life cycle.

A limited number of studies have calculated the life-cycle footprints of ships using individual product data and sectoral statistics. Such studies have estimated the embodied impact based on the material inventory of a single ship and used sectoral statistics for ship operation (Chatzinikolaou & Ventikos, 2015; Kjær et al., 2015; Ringvold, 2017). However, this modeling approach has two limitations. First, the material inventory of a ship is usually incomplete and only includes limited categories of materials, such as steel and plastic, while the energy and emission footprints of the shipbuilding process are not usually considered. Second, due to the long operation time, the operational footprint of a ship may dominate its life-cycle impact. Thus, the sectoral statistics relating to ship operation (usually as the average sectoral value) do not usually reflect the conditions of individual ships, and the operational energy and emission footprints should be calculated on a ship-specific basis.

Fortunately, advancements in information and communication technology (ICT) in the maritime industry have offered new opportunities for acquiring ship-specific activity data. The recently introduced automatic identification system (AIS) for vessels provides a promising way to estimate the operational emissions of individual ships at high spatial and temporal resolutions (Corbett, 2016; IMO, 2015, 2021; Johansson et al., 2017; Jonson et al., 2015; Liu et al., 2016, 2019; Olmer et al., 2017; Wang et al., 2021; Zhang et al., 2017, 2019, 2021). AIS data provide real-time ship movement records, allowing us to estimate and track the global emissions of individual ships at high resolution. In addition, global datasets such as the World Register of Ships (WRS) provide information on the engine profiles, structures, and materials of internationally registered ships, which have been used to estimate the embodied footprints of ships in the phases of construction and scrapping (Ringvold, 2017). To ensure a comprehensive system boundary for footprint accounting while maintaining the specificity of product use, the process-based hybrid life-cycle inventory (LCI) modeling approach was developed by Bullard et al. (1978). This approach has been widely used to quantify the footprints of various products and technologies, such as buildings (Chang et al., 2012), shale gas (Chang et al., 2014), and high-speed trains (Chang et al., 2019). As the Chinese government releases input–output (I–O) economic data with fine-scale sectoral detail, the embodied energy and emissions of individual ships can be calculated using the I–O LCI model and the newbuild price of a ship in the WRS database.

This study estimated the life-cycle energy consumption and environmental emissions of individual cargo ships. Unlike previous process-based LCI studies of ships, we used a process-based hybrid LCI modeling approach to calculate the life-cycle footprint on an individual ship basis. Using the economic I–O benchmark of China in 2017, we developed the I–O LCI model for China in a top-down manner. In addition, the high-fidelity data of the AIS and the bottom-up approach were used to estimate the energy consumption and emissions associated with the ship operation phase.

2 | METHODS

In this study, we conducted a life-cycle analysis of cargo ships. As shown in Figure 1, the process-based hybrid LCI modeling approach was used to estimate the primary energy consumption, carbon dioxide (CO_2) emissions, and sulfur dioxide (SO_2) emissions of ships in the phases of raw material extraction and material production, shipbuilding, and ship operation. The estimates were based on the complete boundary of the model for footprint accounting and specific considerations for product use (Chang et al., 2012). Specifically, the I–O LCI model was used to calculate the "cradle-to-plant" (or embodied) energy and emissions associated with the material and fuel use of ship manufacturing. Owing to the advantage of specific considerations for individual products, the process LCI approach along with theoretical calculations was used to quantify the footprint associated with ship operation. The end-of-life phase of a ship was not considered due to the uncertainties associated with future recycling technologies. The functional unit in this study is per unit weight of cargo capacity transported (deadweight tonnage, DWT or dwt) per nautical mile (nm). The energy and emission (CO_2 and SO_2) footprints of ships are reported using the units of joule (J)/nm/DWT and gram (g)/nm/DWT, respectively.

TABLE 1 Newbuilding price by ship type and size

Ship type	Size group (dwt)	Group name	Number of ships	Size (dwt) mean (min, max)	Ship price (million USD) mean (min, max)
Bulk carrier	0–100,000	The small bulk carrier	215	61,758 (20,419, 95,308)	34 (20, 60)
	>100,000	The large bulk carrier	60	240,468 (106,432, 403,784)	77 (44, 133)
Container ship	0–100,000	The small container ship	50	45,765 (11,811, 67,061)	51 (18, 76)
	>100,000	The large container ship	44	122,160 (101,147, 156,694)	108 (82, 167)
General cargo	0–100,000	The small general cargo ship	13	23,298 (5025, 37,472)	28 (12, 42)
	>100,000	The large general cargo ship	0	—	—

Bulk carriers (ships that transport unpackaged bulk cargo, such as grain, coal, and cement), container ships (fully cellular container ships), and general cargo ships (single or multideck cargo vessels for transporting various types of dry cargo) were included in this study. We further categorized ships into small (0—100,000 DWT) and large (>100,000 DWT) subgroups (Table 1) because ship size can affect shipping routes and ship operation at ports. For example, capesize (>100,000 DWT) bulk carriers are generally too large to pass through the Panama Canal and must go round the Cape of Good Hope to travel between the Pacific and Atlantic oceans (Bernacki, 2021). We selected cargo ships that were constructed in shipyards in mainland China between 2011 and 2015, including 275 bulk carriers, 94 container ships, and 13 general cargo ships.

2.1 | LCI modeling of embodied energy and emissions

The "cradle-to-gate" energy and environmental footprints of the selected types of ships were estimated using the I–O LCI model. Derived from the economic I–O method, the I–O LCI model calculates the economy-wide energy and environmental footprint of a given product, avoiding the limited and subjective definition of system boundaries by researchers (Hendrickson et al., 2006). The computational structure of the I–O model can be expressed as

$$e = S(I - A)^{-1}d,$$

where e is the economy-wide environmental footprint; S is the satellite matrix, with $s_{i,j}$ denoting the intensity of sector j for impact i (i.e., the environmental emissions of sector j per unit monetary output); I is the identity matrix; A is a technical coefficient matrix; and d is the final demand vector (Heijungs & Suh, 2002; Hendrickson et al., 1998). The energy and environmental emissions of shipbuilding were calculated by multiplying the monetary value of a vessel by the energy, CO_2 emissions, and SO_2 emissions intensity of the "ships and related devices manufacturing sector" in China's national economic accounts.

In this study, the I–O LCI model was developed based on the economic benchmark data of China in 2017, which consists of 149 sectors. The satellite matrix of the I–O model comprises three footprints: primary energy, CO_2 emissions, and SO_2 emissions. The sectoral energy consumption data, including coal, crude oil, natural gas, and electricity generated by renewable energy, were obtained from the China Statistical Yearbook (NBSC, 2018a). To make the sectoral energy and economic data consistent, the 46-sector energy statistics were split into 149 sectors. Specifically, coal, crude oil, and natural gas consumption were allocated to each sector based on their purchase from the energy production and supply sectors in the I–O table for China. Renewable electricity use was disaggregated based on the output value of the sector. Sectoral CO_2 emissions were primarily estimated using the method proposed by the Intergovernmental Panel on Climate Change (IPCC, 2007). That is, they were based on the energy consumption of each sector (recorded in the China Energy Statistical Yearbook; NBSC, 2018a), CO_2 coefficient of energy use (Dhakal, 2009; IPCC, 2007), and sectoral carbon oxidation factor (SGCCCCS, 2020). Furthermore, the CO_2 emissions of the following high-emission industrial productions were also considered: synthetic ammonia, calcium carbide, and soda ash production associated with the sector of raw chemical materials and chemical product manufacturing; cement production and glass manufacturing associated with the sector of nonmetallic mineral product manufacturing; steelmaking and ironmaking associated with the sector of ferrous metal smelting and rolling processing; and coke production (used as a reducing agent) associated with the sector of ferrous and nonferrous metal smelting and rolling. The production values of these products were obtained from the China Statistical Yearbook (NBSC, 2018b), and reference was made to relevant CO_2 emission coefficients released by the IPCC (2007). Sectoral SO_2 emissions were calculated based on the sectoral energy consumption and SO_2 emission coefficient of each energy type using the method of Peters et al. (2006).

The price information of the selected types of ships was collected from the WRS database (https://ihsmarkit.com), which provides the contract price value (US dollar) of newbuild ships. We converted the price to Chinese yuan using the currency exchange rate released by the World Bank

(The World Bank, 2021), and then adjusted the price to the benchmark year (i.e., 2017) of the I–O LCI model using the producer price index (PPI) in the China Statistical Yearbook (NBSC, 2018c). The results of the I–O LCI model were the embodied energy and emissions of the selected types of ships, including the footprint associated with shipbuilding. However, to classify the energy consumption and emissions by the life-cycle phase of a vessel, we subtracted the value of shipbuilding from the I–O model result to yield the footprint associated with the upstream supply chain of a ship. The energy and environmental footprints of shipbuilding were calculated by multiplying the monetary value of a vessel by the corresponding intensity of CO_2 and SO_2 emissions and related device manufacturing sectors.

2.2 | AIS-based modeling of operational emissions

We estimated the operational energy use and emissions of each ship using a power-based calculation and the AIS data by following the emission model and emission factors of Zhang et al. (2019, 2021). We calculated the operational emissions of maritime shipping under two policy scenarios: pre-2019 and post-2020. In the pre-2019 scenario, ships operated by following emission policies that were implemented prior to 2019, including the 0.1% sulfur limit mandated in the four IMO-delegated emission control areas (ECAs) (IMO, 2017) and the regulations included in the sulfur directive for European ports (European Parliament, 2003). Other than in areas affected by the 0.1% sulfur cap, we assumed that ships used heavy fuel oil (HFO) with a sulfur content of 2.7%. In the post-2020 scenario, ships operated by following the policies relevant to 2020. That is, they used marine diesel oil (MDO) with a 0.5% sulfur limit according to the global sulfur cap introduced in 2020 (IMO, 2017). We did not consider local policies in the transitional period during 2019, such as the 0.5% sulfur cap implemented in Chinese domestic emission control areas (DECAs) or selected ports within DECAs before the global sulfur cap of 0.5% in 2020 (MOT, 2015, 2018). The estimated energy consumption and emissions in the ship operation phase were aggregated into either moving mode (i.e., AIS signals showing a nonzero ship speed) or berthing mode. For the moving mode, both propulsion engines and auxiliary engines were in operation. For the berthing mode, we assumed that propulsion engines were turned off, whereas auxiliary engines were still in operation if the AIS was still online.

Raw data from the AIS in 2015 were used to estimate the annual energy consumption and atmospheric emissions associated with operating ships. Ship parameters (including engine parameters) were collected from the WRS database. Auxiliary engine and boiler engine loads were obtained from the IMO study on greenhouse gases (GHG) (IMO, 2015).

3 | RESULTS AND DISCUSSION

3.1 | Embodied energy consumption and emissions

The embodied energy, CO_2 emissions, and SO_2 emissions of the selected types of ships are summarized in Table 2. Overall, container ships had the highest embodied footprint, followed by bulk carriers and general cargo ships. Large (>100,000 DWT) container ships had the largest average embodied energy (1010 TJ), followed by large bulk carriers (767 TJ), small (0–100,000 DWT) container ships (494 TJ), small bulk carriers (329 TJ), and small general cargo ships (267 TJ). The embodied CO_2 and SO_2 emissions ranked in the same order. Large container ships had the highest average embodied CO_2 emissions (108,688 t), which were 32% higher than those of large bulk carriers (82,477 t). For ship groups with capacities of <100,000 DWT, the average CO_2 emissions of container ships (53,135 t) were 50% higher than those of bulk carriers (35,419 t) and 85% higher than those of general cargo ships (28,770 t). In addition, the average SO_2 emissions of large container ships (234 t) were nearly 3 times higher than those of small general cargo ships.

For the three ship types (i.e., bulk carrier, container ship, and general cargo ship), their embodied footprints were dominated by the material stage (including raw material extraction and material production). The material stage accounted for 94% and 97% of the embodied energy and CO_2 footprints, respectively, whereas shipbuilding accounted for just 3–6%. Shipbuilding only accounted for 0.2% of the embodied SO_2 footprint because the energy consumption of shipyards mainly relies on natural gas (especially liquefied natural gas) and electricity. Although gas and electric power account for ~91% of the total end-use energy of the shipbuilding sector in China (NBSC, 2019), the onsite use of natural gas and electricity in shipyards does not emit SO_2. The significant contribution of CO_2 emissions during the material stage to the embodied footprint of ships indicates that the key to ship decarbonization lies in utilizing low-carbon energy throughout China's industrial system. This highlights the urgent need for shipbuilders and policymakers to focus on managing the mitigation of supply-chain carbon.

The embodied energy and emissions of a given type of ship varied significantly by ship size. As the embodied energy and environmental footprints estimated by the I–O LCI model exhibited linear relationships with the monetary value of a vessel product, the relationship between ship size and embodied footprint could be analyzed using the price–size curve (Figure S1 in the Supporting Information). The logarithmic growth curves of the three ship types revealed an analogical effect of economies of scale, that is, the price of a vessel did not proportionally increase (but increased slowly) with an increase in vessel weight, suggesting a diminishing marginal environmental footprint with increasing vessel size. As a result, ships with larger DWT should be given priority under future requirements associated with the increasing capacity and upgrading of the waterborne

TABLE 2 Embodied energy and emissions of cargo ships by ship type, size, and LCA phase

Measures mean (min, max)	Ship type	Size (dwt)	Material	Shipbuilding	Total (material + shipbuilding)
Energy (GJ)	Bulk carrier	0–100,000	307,989 (170,457, 608,926)	21,367 (11,826, 42,245)	329,356 (182,283, 651,170)
		>100,000	717,191 (365,859, 1,218,595)	49,755 (25,382, 84,541)	766,946 (391,241, 1,303,136)
	Container	0–100,000	462,047 (152,453, 696,340)	32,055 (10,576, 48,309)	494,101 (163,029, 744,649)
		>100,000	945,118 (685,986, 1,530,115)	65,568 (47,591, 106,153)	1,010,686 (733,577, 1,636,268)
	General cargo	0–100,000	250,176 (108,200, 384,819)	17,356 (7506, 26,697)	267,532 (115,706, 411,516)
		>100,000	—	—	—
CO_2 (metric tons)	Bulk carrier	0–100,000	34,307 (18,988, 67,829)	1111 (615, 2197)	35,419 (19,603, 70,026)
		>100,000	79,889 (40,754, 135,741)	2588 (1320, 4396)	82,477 (42,074, 140,138)
	Container	0–100,000	51,468 (16,982, 77,566)	1667 (550, 2512)	53,135 (17,532, 80,079)
		>100,000	105,278 (76,413, 170,442)	3410 (2475, 5520)	108,688 (78,888, 175,963)
	General cargo	0–100,000	27,867 (12,053, 42,866)	903 (390, 1388)	28,770 (12,443, 44,254)
		>100,000	—	—	—
SO_2 (ton)	Bulk carrier	0–100,000	76 (42, 151)	0.181 (0.100, 0.357)	76 (42, 151)
		>100,000	177 (91, 302)	0.420 (0.214, 0.714)	178 (91, 302)
	Container	0–100,000	114 (38, 172)	0.271 (0.089, 0.408)	115 (38, 173)
		>100,000	234 (170, 379)	0.554 (0.402, 0.897)	234 (170, 380)
	General cargo	0–100,000	62 (27, 95)	0.147 (0.063, 0.226)	62 (27, 95)
		>100,000	—	—	—

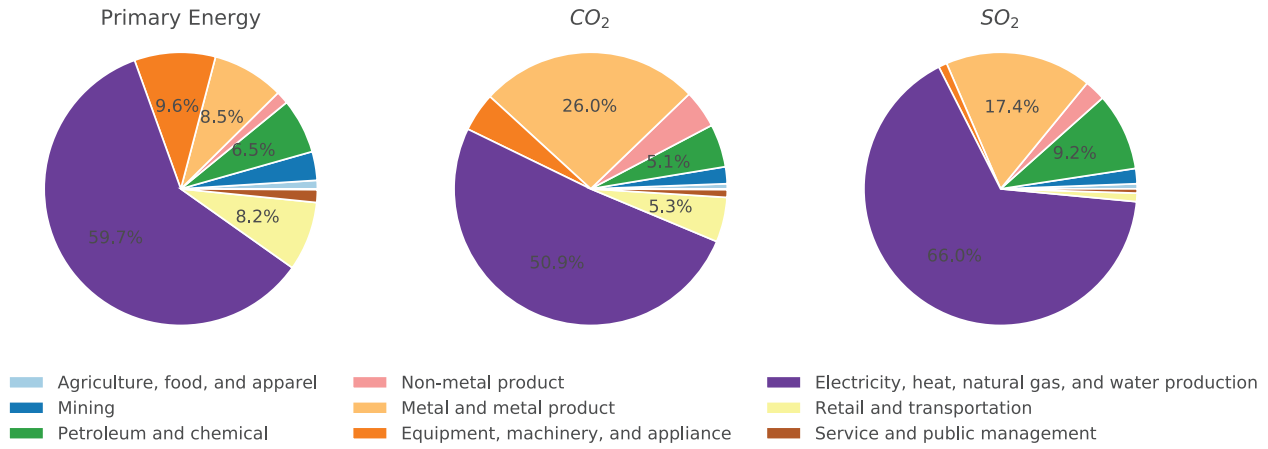

FIGURE 2 Structure of the embodied footprints of shipbuilding. Underlying data for this figure can be found in the Supporting Information

transport sector. Larger ships could help achieve economies of scale and reduce emissions and costs associated with sea transport. The ability to accommodate ever-larger ships has been a positive indicator of port infrastructure and efficiency. Statistics have shown that the average (per port) size of the largest ship increased by 125% between 2006 and 2020 (Hoffmann & Hoffman, 2021). In the long term, this would require ports to build their capacity (e.g., by constructing new terminals, retrofitting outdated infrastructure, and deepening harbors) to serve larger cargo vessels. Moreover, to achieve increasing environmental returns, larger carrying capacities should be preferentially deployed by the busiest shipping routes of global trade.

Figure 2 shows the contributions of the source sectors to the embodied footprint of each type of ship. Owing to the high reliance on electricity in the industrial sectors of China's economic system, the sector of power, heat, gas, and water production made the highest contribution (51–66% by footprint category) to vessels' supply-chain energy and emission footprints. This finding highlights the need for a lower-carbon transition of the country's power supply. Fortunately, the Chinese government has made considerable efforts to accelerate the use of green power via the massive deployment of renewable electricity generation technologies (e.g., wind and solar farms), which is one of the crucial pathways to reach China's carbon neutrality pledge by 2060 (Yang et al., 2020). The metal manufacturing sector also made a large contribution (10–26%) to the embodied

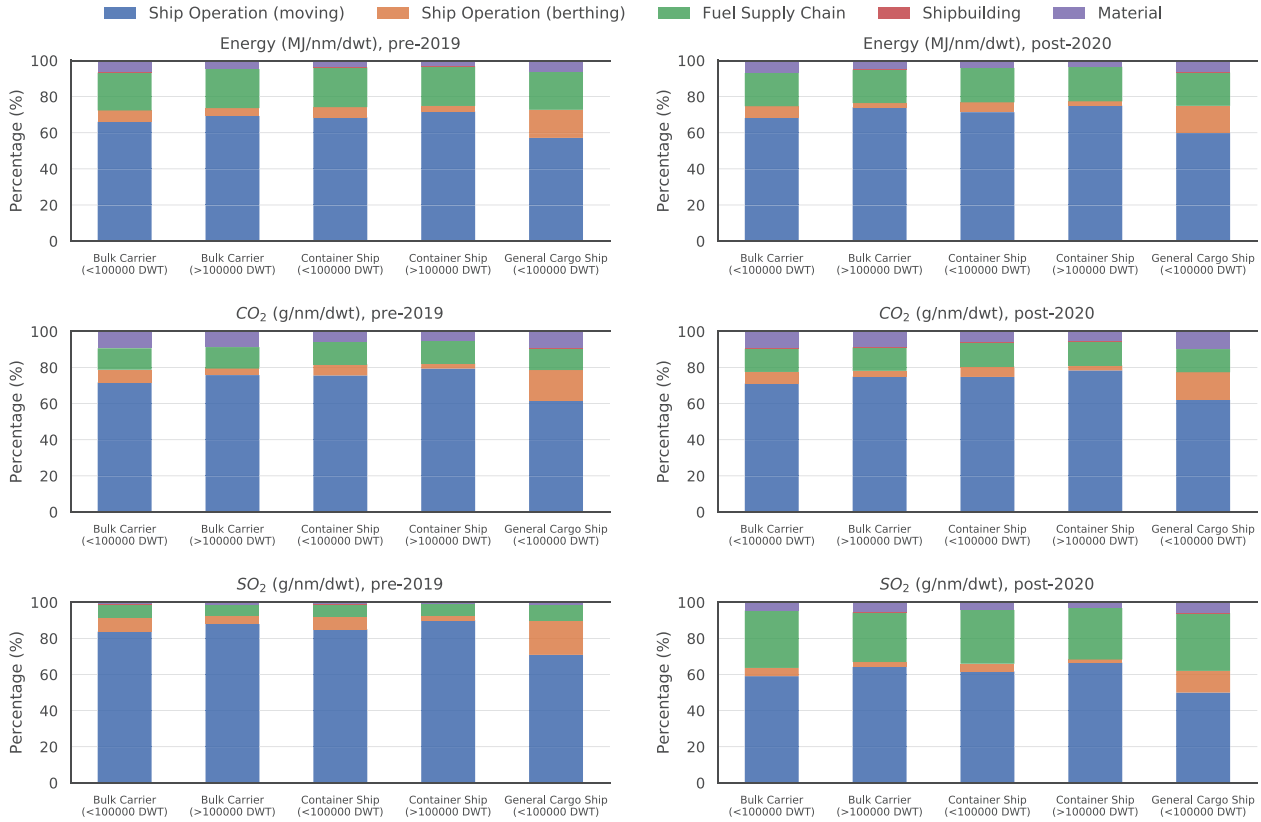

FIGURE 3 Life-cycle footprints of cargo ships by ship type, size, and LCA phase (pre-2019 policy scenario vs. post-2020 policy scenario). Underlying data for this figure can be found in the Supporting Information

footprints of ships. As steel manufacturing is energy intensive and has high emissions, reducing the heavy use of steel in shipbuilding could help mitigate the embodied energy and emissions of ships. For example, the lightweight construction of vessels using advanced composite materials (e.g., fiber-reinforced polymer) would reduce our reliance on steel and aluminum, thus alleviating the embodied CO_2 and SO_2 emissions of ships (Evegren et al., 2011). Furthermore, as the massive transportation of raw materials also consumes energy and emits pollutants, the retail and transportation sector also made noticeable contributions to the embodied energy (8%) and CO_2 emission footprints (5.3%) of ships. Thus, embodied CO_2 footprints could be reduced if shipyards purchase steel locally and transition to low-carbon road and railway transport (via grid decarbonization and diesel fuel substitution with biodiesel and/or liquefied natural gas). Owing to their fundamental roles in the industrial system (i.e., a fuel and feedstock supplier to other sectors), the petroleum, chemical, and mining sectors also contributed to the embodied footprints of ships. In contrast, the agriculture, food, and service sectors made nonsignificant contributions to the estimated embodied footprints.

3.2 | Life-cycle footprints

As illustrated in Figure 3, ship usage, which includes the phases of ship moving, ship berthing, and the fuel supply chain (the process of fuel production and delivery), dominated the life-cycle energy consumption and environmental emissions of ships. Assuming a uniform lifespan of 20 years, the levelized energy consumption of ship production (material production and shipbuilding) only contributed 3–7% to the entire life-cycle process, whereas the fuel supply chain contributed 20–22% and ship operation (moving and berthing) contributed 72–75%. Regarding the "cradle-to-propeller" energy consumption of ships, the operational energy contributions of container ships and bulk carriers were similar (66–72%) in moving mode, whereas that of small general cargo ships was 57%.

For ship berthing, small general cargo ships contributed the most (15%) to the total energy use, whereas other types of ships contributed 3–6%. In addition, CO_2 emissions exhibited the same ranking as energy consumption. The phase of ship production only contributed 5–9% to the life-cycle CO_2 emissions, whereas the phase of ship use contributed >90%. Specifically, for container ships and bulk carriers, ship operation in moving mode contributed 71–79% of the life-cycle CO_2 emissions, whereas ship operation in berthing mode contributed 2–7%. For small general cargo ships, ship operation in moving mode and berthing mode contributed 61% and 16% of life-cycle CO_2 emissions, respectively.

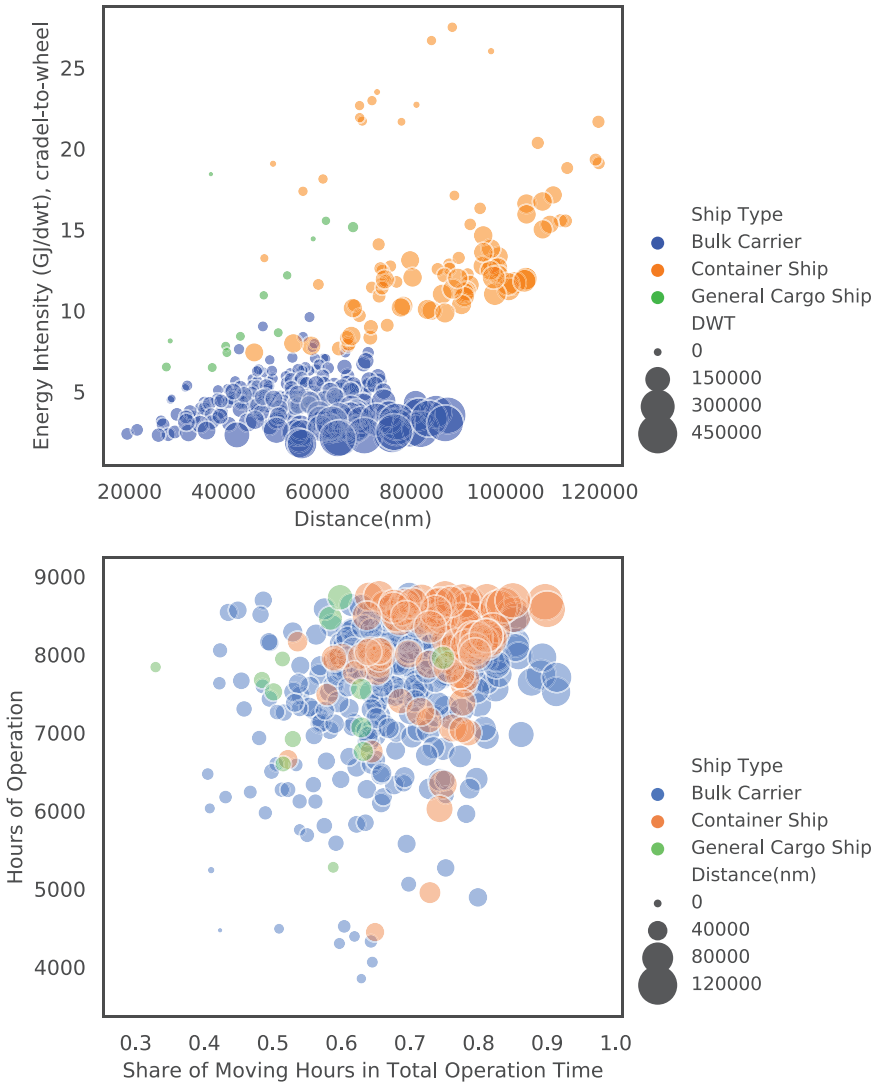

FIGURE 4 Energy intensities associated with the activity profiles of different types of ships

As shown in Table 3, in terms of the absolute value of energy consumption, large (>100,000 DWT) bulk carriers were the most energy efficient, with the lowest average life-cycle energy intensity (46 MJ/nm/1000 DWT) under the pre-2019 policy scenario, followed by small (0–100,000 DWT) bulk carriers (96 MJ/nm/1000 DWT), large container ships (133 MJ/nm/1000 DWT), and small container ships (196 MJ/nm/1000 DWT). Small general cargo ships turn out to be the least energy efficient, with an averaged energy intensity of 238 MJ/nm/1000 DWT.

These findings are attributable to the operational profiles of these ships. Figure 4 shows that a linear relationship was observed between the energy intensity by weight (GJ/DWT) and distance traveled (nm); however, there were variations among the different types of ships in terms of the ratio of these two parameters. Overall, bulk carriers had a higher energy efficiency (lower energy intensity when traveling the same distance) than container ships, and ships with larger capacities (DWT) exhibited higher energy efficiencies than ships with lower capacities. Although small general cargo ships and small container ships had similar operational energy intensities of approximately 134 and 131 MJ/nm/1000 DWT, respectively, small general cargo ships had a higher energy intensity (37 MJ/nm/1000 DWT) in berthing mode than small container ships (11 MJ/nm/1000 DWT). These two types of ships are within the same size category and transport similar types of cargo; however, they have different levels of cargo packaging, thus affecting the efficiency of port activities. Our results indicate that the use of containers could increase the efficiency of cargo loading or unloading at ports, which could increase the energy efficiency (shorter time spent) of port activities and lower the life-cycle energy footprint.

The distance traveled is a critical factor when calculating the levelized energy intensity (MJ/nm/DWT) for the stages of material and shipbuilding. The distance traveled is associated with annual operation time and the time allocation for port activities. As shown in Figure 4, more operation hours coupled with a higher share of moving hours in the total operation time would lead to a longer traveled distance, and a longer distance would result in a lower levelized energy intensity (MJ/nm/DWT) when other conditions remain the same. In this study, container ships and bulk carriers clustered in areas with an annual operation time of >8000 h (i.e., >91% of the total hours in a calendar year), while berthing time represented <30% of the total operational hours. The point distribution of general cargo ships was less concentrated than the point distribution of other types of ships. There were general cargo ships with <6000 h of operation time or with <40% of their operation time allocated to moving, leading to a very small distance.

TABLE 3 Life-cycle footprints of cargo ships by ship type, size, and LCA phase

					Operation (pre-2019)			Operation (post-2020)				
						Ship operation			Ship operation			
Measure	Ship type	Size (dwt)	Material	Shipbuilding	Fuel supply chain	Moving	Berthing	Fuel supply chain	Moving	Berthing	Total (pre-2019)	Total (post-2020)
Energy (MJ/ nm/1000 dwt)	Bulk carrier	0–100,000	6	0.382	20	63	6	17	63	6	96	91
			(2, 17)	(0.156, 1)	(12, 37)	(37, 135)	(2, 15)	(10, 34)	(36, 135)	(1, 14)	(57, 187)	(53, 187)
		>100,000	2	0.170	10	32	2	8	32	1	46	44
			(1, 9)	(0.098, 0.593)	(7, 14)	(21, 43)	(0.173, 8)	(5, 12)	(21, 43)	(0.154, 8)	(31, 71)	(29, 67)
	Container ship	0–100,000	7	0.479	43	134	11	35	131	10	196	183
			(3, 21)	(0.226, 1)	(25, 82)	(75, 234)	(2, 60)	(20, 64)	(72, 234)	(2, 54)	(117, 377)	(108, 345)
		>100,000	4	0.295	29	95	4	24	94	3	133	126
			(3, 7)	(0.206, 0.476)	(24, 37)	(80, 120)	(2, 8)	(20, 30)	(79, 120)	(2, 7)	(112, 165)	(107, 157)
	General cargo ship	0–100,000	14	0.957	50	136	37	41	134	33	238	223
			(8, 29)	(0.527, 2)	(36, 92)	(84, 289)	(16, 83)	(28, 92)	(81, 289)	(14, 83)	(167, 494)	(154, 494)
		>100,000	–	–	–	–	–	–	–	–	–	–
CO_2 (g/nm/ 1000 dwt)	Bulk carrier	0–100,000	613	20	808	4866	477	848	4693	420	6784	6594
			(251, 1848)	(8, 60)	(471, 1733)	(2868, 10,131)	(119, 1183)	(492, 1733)	(2729, 10,131)	(103, 1058)	(4036, 13,596)	(3878, 13,596)
		>100,000	273	9	387	2462	117	412	2380	102	3249	3175
			(157, 952)	(5, 31)	(257, 557)	(1600, 3310)	(13, 656)	(274, 584)	(1540, 3205)	(12, 565)	(2183, 5232)	(2119, 5034)
	Container ship	0–100,000	770	25	1696	10,383	859	1758	9838	765	13,732	13,155
			(363, 2358)	(12, 76)	(980, 3168)	(5826, 17,696)	(171, 4632)	(1004, 3224)	(5410, 17,573)	(157, 4067)	(8290, 26,734)	(7831, 25,095)
		>100,000	474	15	1154	7376	269	1217	7090	248	9288	9044
			(331, 764)	(11, 25)	(966, 1441)	(6192, 9318)	(141, 584)	(1018, 1527)	(5940, 8991)	(132, 515)	(7913, 11,452)	(7700, 11,198)
	General cargo ship	0–100,000	1537	50	2043	10,465	2861	2082	10,069	2485	16,956	16,221
			(847, 3216)	(27, 104)	(1398, 4629)	(6508, 21,700)	(1249, 6268)	(1415, 4629)	(6114, 21,700)	(1069, 6210)	(11,876, 35,859)	(11,218, 35,859)
		>100,000	–	–	–	–	–	–	–	–	–	–
SO_2 (g/ nm/1000 dwt)	Bulk carrier	0–100,000	1	0.003	7	77	7	7	13	1	91	23
			(0.557, 4)	(0.001, 0.010)	(4, 13)	(6, 156)	(0.192, 17)	(4, 13)	(6, 27)	(0.192, 3)	(22, 175)	(14, 41)
		>100,000	0.607	0.001	3	41	2	3	7	0.295	47	11
			(0.349, 2)	(0.001, 0.005)	(2, 5)	(27, 56)	(0.227, 11)	(2, 5)	(5, 10)	(0.035, 2)	(32, 69)	(8, 17)
	Container ship	0–100,000	2	0.004	14	166	13	14	29	2	195	46
			(0.806, 5)	(0.002, 0.012)	(8, 26)	(11, 297)	(0.678, 79)	(8, 25)	(11, 51)	(0.342, 12)	(39, 390)	(28, 89)
		>100,000	1	0.002	9	119	3	9	21	0.541	132	32
			(0.736, 2)	(0.002, 0.004)	(8, 12)	(98, 151)	(1, 10)	(8, 12)	(17, 26)	(0.237, 2)	(109, 166)	(27, 40)
	General cargo ship	0–100,000	3	0.008	17	141	38	16	25	6	199	51
			(2, 7)	(0.004, 0.017)	(12, 36)	(13, 193)	(4, 106)	(11, 36)	(13, 34)	(3, 16)	(60, 240)	(40, 60)
		>100,000	–	–	–	–	–	–	–	–	–	–

Note: Assuming that lifespan of a ship is 20 years.

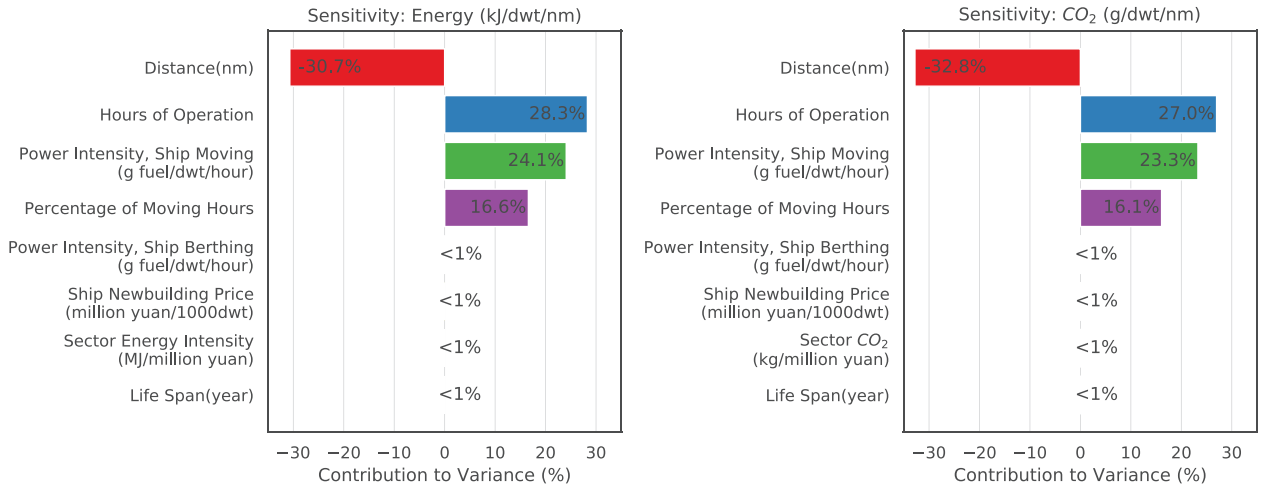

FIGURE 5 Sensitivity analysis of LCA estimates in this study

Note that the sample size of general cargo ships was much smaller than that of other types of ships, thus affecting the comparability of the results to a certain extent.

The global sulfur cap of 0.5% introduced in 2020 led to obvious changes in the amounts of ship emissions and the emission shares by phases (Tables S2 and S3). In the post-2020 scenario, the CO_2 emissions relating to ship operation (moving and berthing) decreased by 4–6% compared with the pre-2019 scenario, whereas the CO_2 emissions relating to the fuel supply chain increased by 2–6%. Such changes can be attributed to the combined effect of lower values of specific fuel oil consumption (SFOC, g fuel/kWh) and larger emission factors (g CO_2/g fuel) for the lower-sulfur fuel used in the post-2020 scenario (IMO, 2015). Consequently, the global sulfur cap of 0.5% led to a 2–4% reduction in the cradle-to-propeller CO_2 emissions of ships.

For SO_2 emissions, the global sulfur cap led to a dramatic decrease in emissions and an obvious change in the emission shares by phase. In the pre-2019 scenario, the intensity of cradle-to-propeller SO_2 emissions ranged from 47 to 199 g/nm/1000 DWT, with ship operation contributing 90–92%. Compared with the pre-2019 scenario, SO_2 emissions in the ship operation phase decreased by 82–83% in the post-2020 scenario. In the post-2020 scenario, we assumed that ships used MDO with a sulfur content of 0.5%, for which the emission factor was ~83% lower than that of HFO with a sulfur content of 2.7% in the pre-2019 scenario. With the decreased emission amount, there was a reduction in the contribution of SO_2 emissions in the ship operation phase to the total SO_2 emissions in the LCA, whereas the contributions of the material, shipbuilding, and fuel supply-chain phases increased. From the pre-2019 scenario to the post-2020 scenario, the proportion of levelized embodied SO_2 emissions increased from 0.8–1.5% to 3–6%, while the share of emissions from the fuel supply chain increased from 6–8% to 27–32%. Consequently, the global sulfur cap of 0.5% reduced the cradle-to-propeller SO_2 emissions of ships by >90%. There was more potential to reduce emissions in berthing mode than in moving mode due to the different movements of shipping activities in ECAs and European ports that already mandated a 0.1% sulfur limit in the pre-2019 scenario. Ships that already operated for long periods in areas with a sulfur cap were less affected by the new global sulfur cap; thus, they achieved smaller emission reductions between the pre-2019 and post-2020 scenarios. Spatial maps of emissions for the different types of ships are provided in Figure S2.

3.3 | Sensitivity analysis

Figure 5 presents the results of the sensitivity analysis for the cradle-to-propeller energy consumption and CO_2 emissions of ships. The sensitivity analysis was performed using Oracle Crystal Ball (with 500,000 trial runs), which is commonly used for sensitivity and uncertainty analyses in LCA research (Chang et al., 2019; Wang et al., 2017). Overall, the results showed that the two impact categories had similar sensitive factors. The travel distance of a ship was the largest contributor to the variabilities in the impacts of energy and CO_2 emissions (30.7% and 32.8%, respectively), followed by the total hours of ship operation (28.3% and 27.0%, respectively), operational power intensity in moving mode (24.1% and 23.3%, respectively), and the share of moving hours in the total operation time (16.6% and 16.1%, respectively). These findings relate to the fact that energy consumption and CO_2 emissions during ship operation dominated the life-cycle footprint of ships, contributing >90% of the total.

The operation of a vessel includes moving (i.e., sailing) and berthing. The fuel consumption during berthing is significantly lower than that during sailing because propulsion engines are shut down. In addition, as the ratio of sailing time to berthing time varies by ship type, ships with a longer lifespan do not necessarily have a longer travel distance. As a result, the share of moving hours in the total operation time was also an obvious

contributor to the variance in energy and CO_2 emissions. In contrast, the lifespan and berthing power intensity of a ship had little effect on the cradle-to-propeller results. Similarly, the model parameters relating to the embodied energy and CO_2 emissions of ships (e.g., newbuilding price and the intensity of sectoral CO_2 emissions) made negligible contributions to the variability in the results.

For the model developed in this study, the processed data of ship operation (including operational power intensity, operation time, and traveled distance) were estimated based on high-fidelity marine traffic data and engine profiles obtained from the official dataset of ship registration, which is based on individual ships and reflects actual practice. The embodied energy and emissions of ships determined by the I–O LCI model reflect the national average level of production of the material sectors. Although the life-cycle impacts of ships are insensitive to their embodied footprints, uncertainties relating to the embodied energy and emissions of specific industrial processes determine the extent to which the low-carbon opportunities associated with ship delivery can be unlocked. Thus, more robust analyses that are specific to the supply chain of ship building (Laner et al., 2014; Salemdeeb et al., 2021) should be included in future studies.

4 | CONCLUSIONS

This study quantified the life-cycle energy consumption and environmental emissions of cargo ships using the hybrid LCI modeling approach. Compared with other studies, our estimations have several advantages. First, we established a complete system boundary for life-cycle footprint accounting. As the I–O LCI model calculated the energy and environmental footprint of products throughout the economic system, our results of the embodied footprints of ships were not constrained by the limited data of shipbuilding materials and processes, nor a subjective definition of the system boundaries. Overall, the embodied footprints, accounting for <10% of the cradle-to-propeller footprints of ships, were dominated by raw material production. In this case, there are opportunities for decarbonization by mitigating supply-chain carbon and using low-carbon energy throughout China's industrial system. Although the end-of-life phase of ships was not considered in this study, primarily due to scarce data on current practice and the high uncertainty associated with future recycling technologies, the recycling and reuse of ships is a critical pathway for reducing embodied footprints. Promoting the recycling and reuse of ships helps society to transition toward a circular economy, which is a multidimensional process across political, social, environmental, economic, and technical domains (Awasthi et al., 2021). To better embed the marine-shipping industry in the circular economy, more efforts should be placed on building a more integrated supply chain across the life-cycle stages of maritime shipping and developing closer collaborations among stakeholders (OECD, 2019).

Second, based on our unique dataset, our findings provide a comprehensive understanding of the life-cycle footprints of cargo transport. A total of 382 ships, covering three of the most important types of cargo ships, were included in our estimations. Using ship-by-ship marine traffic data and parameter data such as engine specifications, ship capacities, and newbuilding prices, we estimated the cradle-to-propeller footprints on an individual ship basis. Such estimation allows us to examine the footprints of different life-cycle stages according to the characteristics and activity profiles of different types of ships. Among the three types of ships considered in this study, we found that bulk carriers were the most energy efficient, and that ships with larger capacities (DWT) had higher energy efficiencies than ships with lower capacities. Compared with general cargo ships, container ships had higher energy efficiency during ship berthing, indicating that the use of containers could help increase the efficiency of port activities, thus advancing the transition to energy-efficient maritime shipping. Although the results of this study are based on cargo ships that were built in mainland China between 2011 and 2015, the methodological framework of our estimations could be applied to wider spatial and temporal scales, depending on data availability.

Moreover, this study presents the energy and environmental footprints of ships under the new policy scenario of the 2020 global sulfur cap. We found that the sulfur cap dramatically decreased SO_2 emissions during ship operation, thus changing the SO_2 emission contributions of other life-cycle stages when transitioning from HFO to MDO. Although the sulfur cap targets improvements in air quality and public health, our estimates indicate that it would also slightly reduce the life-cycle CO_2 footprint, implying the co-benefit for mitigating GHG emissions.

ACKNOWLEDGMENTS

Yiqi Zhang acknowledges support from the RGC Postdoctoral Fellowship Scheme (PDFS2122-6S09). The AIS data used in this study are managed by the Institute for the Environment (IENV) and the Environmental Central Facility (ENVF) of the Hong Kong University of Science and Technology (HKUST).

CONFLICT OF INTEREST

The authors declare no conflict of interest.

DATA AVAILABILITY STATEMENT

The data that supports the findings of this study are available in this article.

ORCID

Yiqi Zhang https://orcid.org/0000-0003-1795-7450
Yuan Chang https://orcid.org/0000-0002-9790-4529
Jimmy C. H. Fung https://orcid.org/0000-0002-7859-8511
Alexis K. H. Lau https://orcid.org/0000-0003-3802-828X

REFERENCES

Awasthi, A. K., Cheela, V. R. S., D'Adamo, I., Iacovidou, E., Islam, M. R., Johnson, M., & Li, J. (2021). Zero waste approach towards a sustainable waste management. *Resources, Environment and Sustainability*, *3*, 100014. https://doi.org/10.1016/j.resenv.2021.100014

Bernacki, D. (2021). Assessing the link between vessel size and maritime supply chain sustainable performance. *Energies*, *14*(11). https://doi.org/10.3390/en14112979

Bullard, C. W., Penner, P. S., & Pilati, D. A. (1978). Net energy analysis-handbook for combining process and input-output analysis. *Resource Energy*, *1*(3), 267–313.

Chang, Y., Huang, R. Z., Ries, R., & Masanet, E. (2014). Shale-to-well energy use and air pollutant emissions of shale gas production in China. *Applied Energy*, *125*, 147–157. https://doi.org/10.1016/j.apenergy.2014.03.039

Chang, Y., Lei, S., Teng, J., Zhang, J., Zhang, L., & Xu, X. (2019). The energy use and environmental emissions of high-speed rail transportation in China: A bottom-up modeling. *Energy*, *182*, 1193–1201. https://doi.org/10.1016/j.energy.2019.06.120

Chang, Y., Ries, R., & Lei, S. H. (2012). The embodied energy and emissions of a high-rise education building: A quantification using process-based hybrid life cycle inventory model. *Energy and Buildings*, *55*, 790–798. https://doi.org/10.1016/j.enbuild.2012.10.019

Chatzinikolaou, S. D., & Ventikos, N. P. (2015). Holistic framework for studying ship air emissions in a life cycle perspective. *Ocean Engineering*, *110*, 113–122. https://doi.org/10.1016/j.oceaneng.2015.05.042

Corbett, J. (2016). Transport: Shipping emissions in East Asia. *Nature Climate Change*, *6*, 983–984. https://doi.org/10.1038/nclimate3091

Dhakal, S. (2009). Urban energy use and carbon emissions from cities in China and policy implications. *Energy Policy*, *37*(11), 4208–4219. https://doi.org/10.1016/j.enpol.2009.05.020

European Parliament. (2003). *Directive 2003/17/EC of the European Parliament and of the Council of 3 March 2003 amending Directive 98/70/EC relating to the quality of petrol and diesel fuels*. https://eur-lex.europa.eu/legal-content/en/ALL/?uri=CELEX%3A32003L0017

Evegren, F., Hertzberg, T., & Rahm, M. (2011). *Lightweight construction of a cruise vessel*. https://www.diva-portal.org/smash/get/diva2:962601/FULLTEXT01.pdf

Heijungs, R., & Suh, S. (2002). *The computational structure of life cycle assessment*. Kluwer Academic Publishers.

Hendrickson, C., Horvath, A., Joshi, S., & Lave, L. (1998). Economic input-output models for environmental life-cycle assessment. *Environmental Science and Technology*, *32*(7), 184A–191A. https://doi.org/10.1021/es983471i

Hendrickson, C. T., Lave, L. B., & Matthews, H. S. (2006). *Environmental life cycle assessment of goods and services: An input–output approach*. RFF Press.

Hoffmann, J., & Hoffman, J. (2021). *Bigger ships and fewer companies—Two sides of the same coin*. https://unctad.org/news/bigger-ships-and-fewer-companies-two-sides-same-coin#_edn1

International Maritime Organization. (2015). *Third IMO Greenhouse Gas Study 2014*. 1–26. https://www.imo.org/en/OurWork/Environment/Pages/Greenhouse-Gas-Studies-2014.aspx

International Maritime Organization. (2017). *Sulphur oxides (SOx)—Regulation 14*. http://www.imo.org/en/OurWork/Environment/PollutionPrevention/AirPollution/Pages/Sulphur-oxides-(SOx)-–-Regulation-14.aspx

International Maritime Organization. (2018). *Initial IMO strategy on reduction of GHG emissions from ships*. https://www.imo.org/en/MediaCentre/HotTopics/Pages/Reducing-greenhouse-gas-emissions-from-ships.aspx

International Maritime Organization. (2021). Fourth IMO Greenhouse Gas Study. In *International Maritime Organization* (Vol. 6). https://www.imo.org/en/OurWork/Environment/Pages/Fourth-IMO-Greenhouse-Gas-Study-2020.aspx

IPCC. (2007). *2006 IPCC guidelines for national greenhouse gas inventories*. National Greenhouse Gas Inventories Programme. Institute for Global Environmental Strategies (IGES).

Johansson, L., Jalkanen, J. P., & Kukkonen, J. (2017). Global assessment of shipping emissions in 2015 on a high spatial and temporal resolution. *Atmospheric Environment*, *167*, 403–415. https://doi.org/10.1016/j.atmosenv.2017.08.042

Jonson, J. E., Jalkanen, J. P., Johansson, L., Gauss, M., & Van Der Gon, H. A. C. D. (2015). Model calculations of the effects of present and future emissions of air pollutants from shipping in the Baltic Sea and the North Sea. *Atmospheric Chemistry and Physics*, *15*(2), 783–798. https://doi.org/10.5194/acp-15-783-2015

Kjær, L. L., Pagoropoulos, A., Hauschild, M., Birkved, M., Schmidt, J. H., & McAloone, T. C. (2015). From LCC to LCA using a hybrid input output model—A maritime case study. *Procedia CIRP*, *29*, 474–479. https://doi.org/10.1016/j.procir.2015.02.004

Laner, D., Rechberger, H., & Astrup, T. (2014). Systematic evaluation of uncertainty in material flow analysis. *Journal of Industrial Ecology*, *18*(6), 859–870. https://doi.org/10.1111/jiec.12143

Liu, H., Fu, M., Jin, X., Shang, Y., Shindell, D., Faluvegi, G., Shindell, C., & He, K. (2016). Health and climate impacts of ocean-going vessels in East Asia. *Nature Climate Change*, *6*, 1037–1041. https://doi.org/10.1038/nclimate3083

Liu, H., Meng, Z. H., Lv, Z. F., Wang, X. T., Deng, F. Y., Liu, Y., & He, B. K. (2019). Emissions andhealth impacts from global shipping embodied in US–China bilateral trade. *NatureSustainability*, *2*(11), 1027–1033. https://doi.org/10.1038/s41893-019-0414-z

Ministry of Transport of the People's Republic of China. (2015). *Marine emission control area plan for Pearl River Delta, Yangtzy River Delta, Bohai Rim Area*. http://www.gov.cn/xinwen/2015-12/04/content_5019932.htm

Ministry of Transport of the People's Republic of China. (2018). *Implementation scheme of the domestic emission control areas for atmospheric pollution from vessels*. https://www.msa.gov.cn/public/documents/document/mtex/mzm1/~edisp/20181219111335546.pdf

NBSC (National Bureau of Statistics of China). (2018a). *China Energy Statistical Yearbook 2018*. China Statistics Press.

NBSC (National Bureau of Statistics of China). (2018b). *China Statistical Yearbook 2018*. China Statistics Press.

NBSC (National Bureau of Statistics of China). (2018c). *China Price Statistical Yearbook 2018*. China Statistics Press.

NBSC (National Bureau of Statistics of China). (2019). *China Energy Statistical Yearbook 2019*. China Statistics Press.

OECD. (2019). *Ship recycling: An overview*. https://doi.org/10.1787/397de00c-en

Olmer, N., Comer, B., Roy, B., Mao, X., & Rutherford, D. (2017). *Greenhouse gas emissions from global shipping, 2013–2015* (pp. 1–25). The International Council on Clean Transportation. https://www.theicct.org/sites/default/files/publications/Global-shipping-GHG-emissions-2013-2015_ICCT-Report_17102017_vF.pdf

Peters, G., Weber, C., & Liu, J. 2006. Construction of Chinese energy and emissions inventory; Industrial Ecology Programme Reports and Working Papers[R]. Trondheim, Norway: Norwegian University of Science and Technology, https://ntnuopen.ntnu.no/ntnu-xmlui/bitstream/handle/11250/242545/121799_FULLTEXT01.pdf?sequence=1&isAllowed=y

Ringvold, A. (2017). *Prospective life cycle assessment of container shipping* (pp. 1–82). https://ntnuopen.ntnu.no/ntnu-xmlui/handle/11250/2454930

SGCCCCS (Study Group of China Climate Change Country Study). (2000). *China climate change country study*. Tsinghua University Press.

Salemdeeb, R., Saint, R., Clark, W., Lenaghan, M., Pratt, K., & Millar, F. (2021). A pragmatic and industry-oriented framework for data quality assessment of environmental footprint tools. *Resources, Environment and Sustainability*, *3*, 100019. https://doi.org/10.1016/j.resenv.2021.100019

The World Bank. (2021). *Official exchange rate*. https://data.worldbank.org/indicator/PA.NUS.FCRF

UNCTAD. (2018). *50 years of review of maritime transport, 1968–2018: Reflecting on the past, exploring the future*. https://unctad.org/system/files/official-document/dtl2018d1_en.pdf

Wang, C., Chang, Y., Zhang, L., Pang, M., & Hao, Y. (2017). A life-cycle comparison of the energy, environmental and economic impacts of coal versus wood pellets for generating heat in China. *Energy*, 374–384. https://doi.org/10.1016/jenergy201611085

Wang, X. T., Liu, H., Lv, Z. F., Deng, F.-Y., Xu, H.-L., Qi, L.-J., Shi, M.-S., Zhao, J.-C., Zheng, S.-X., Man, H.-Y., & He, K.-B. (2021). Trade-linked shipping CO_2 emissions. *Nature Climate Change*., *11*, 945–951. https://doi.org/10.1038/s41558-021-01176-6

Yang, J., Zhang, L., Chang, Y., Hao, Y., Liu, G., Yan, Q., & Zhao, Y. (2020). Understanding the material efficiency of the wind power sector in China: A spatial–temporal assessment. *Resources, Conservation and Recycling*, *155*, 104668. https://doi.org/10.1016/j.resconrec.2019.104668

Zhang, Y., Eastham, S. D., Lau, A. K., Fung, J. C., & Selin, N. E. (2021). Global air quality and health impacts of domestic and international shipping. *Environmental Research Letters*, *16*(8), 084055. https://doi.org/10.1088/1748-9326/ac146b

Zhang, Y., Fung, J. C. H., Chan, J. W. M., & Lau, A. K. H. (2019). The significance of incorporating unidentified vessels into AIS-based ship emission inventory. *Atmospheric Environment*, *203*, 102–113. https://doi.org/10.1016/j.atmosenv.2018.12.055

Zhang, Y., Gu, J., Wang, W., Peng, Y., Wu, X., & Feng, X. (2017). Inland port vessel emissions inventory based on ship traffic emission assessment model-automatic identification system. *Advances in Mechanical Engineering*, *9*(7), 1–9. https://doi.org/10.1177/1687814017712878

SUPPORTING INFORMATION

Additional supporting information can be found online in the Supporting Information section at the end of this article.

How to cite this article: Zhang, Y., Chang, Y., Wang, C., Fung, J. C. H., & Lau, A. K. H. (2022). Life-cycle energy and environmental emissions of cargo ships. *Journal of Industrial Ecology*, *26*, 2057–2068. https://doi.org/10.1111/jiec.13293